

PriorGrad: Improving Conditional Denoising Diffusion Models with Data-Driven Adaptive Prior

Sang-gil Lee^{1*} Heeseung Kim¹ Chaehun Shin¹ Xu Tan^{2†} Chang Liu²
 Qi Meng² Tao Qin² Wei Chen² Sungroh Yoon^{1†} Tie-Yan Liu²

¹Data Science & AI Lab., Seoul National University ²Microsoft Research Asia

¹{tkdr1f9202, gmltmd789, chaehun, sryoon}@snu.ac.kr

²{xuta, changliu, meq, taoqin, wche, tyliu}@microsoft.com

Abstract

Denoising diffusion probabilistic models have been recently proposed to generate high-quality samples by estimating the gradient of the data density. The framework assumes the prior noise as a standard Gaussian distribution, whereas the corresponding data distribution may be more complicated than the standard Gaussian distribution, which potentially introduces inefficiency in denoising the prior noise into the data sample because of the discrepancy between the data and the prior. In this paper, we propose PriorGrad to improve the efficiency of the conditional diffusion model (for example, a vocoder using a mel-spectrogram as the condition) by applying an adaptive prior derived from the data statistics based on the conditional information. We formulate the training and sampling procedures of PriorGrad and demonstrate the advantages of an adaptive prior through a theoretical analysis. Focusing on the audio domain, we consider the recently proposed diffusion-based audio generative models based on both the spectral and time domains and show that PriorGrad achieves a faster convergence leading to data and parameter efficiency and improved quality, and thereby demonstrating the efficiency of a data-driven adaptive prior.

1 Introduction

Deep generative models have been achieving rapid progress, by which deep neural networks approximate the data distribution and synthesize realistic samples from the model. There is a wide range of this type of approach, ranging from autoregressive models [24, 25], generative adversarial networks [5, 1], variational autoencoders [14, 39], and normalizing flows [30, 15]. Denoising diffusion probabilistic models (DDPMs) [7] and score matching (SM) [35] are recently proposed categories that can be used to synthesize high-fidelity samples with competitive or sometimes better quality than previous state-of-the-art approaches. Consequently, there have been a variety of applications based on DDPM or SM [32, 12]. Speech synthesis is one of the most successful applications, where the diffusion model can synthesize spectral or time-domain audio conditioned on text or spectral information, respectively, achieving a competitive quality but faster sampling [2, 16, 10, 18] than autoregressive models [25, 11].

However, although the diffusion-based speech synthesis models have achieved high-quality audio generation, they exhibit potential inefficiency, which may necessitate advanced strategies. For example, the model suffers from a significantly slow convergence during training, and a prohibitively

*Work done during an internship at Microsoft Research Asia

†Corresponding Authors

large training computation time is required to learn the approximate reverse diffusion process. We investigate the diffusion-based models and observe the discrepancy between the real data distribution and the choice of the prior. Existing diffusion-based models assume a standard Gaussian as the prior distribution and design a non-parametric diffusion process that procedurally destroys the signal into the prior noise. The deep neural network is trained to approximate the reverse diffusion process by estimating the gradient of the data density. Although applying the standard Gaussian as the prior is simple without any assumptions on the target data, it also introduces inefficiency. For example, in time-domain waveform data, the signal has extremely high variability between different segments such as voiced and unvoiced parts. Jointly modeling the voiced and unvoiced segments with the same standard Gaussian prior may be difficult for the model to cover all modes of the data, leading to training inefficiencies and potentially spurious diffusion trajectories.

Given the above investigation, we assessed the following question: *For a conditional diffusion-based model, can we formulate a more informative prior without incorporating additional computational or parameter complexity?* To investigate this, we propose a simple yet effective method, called PriorGrad, that uses adaptive noise by directly computing the mean and variance for the forward diffusion process prior, based on the conditional information. Specifically, using a conditional speech synthesis model, we propose structuring the prior distribution based on the conditional data, such as a mel-spectrogram for the vocoder [2, 16] and a phoneme for the acoustic model [10]. By computing the statistics from the conditional data at the frame level (vocoder) or phoneme-level (acoustic model) granularity and mapping them as the mean and variance of the Gaussian prior, we can structure the noise that is similar to the target data distribution at an instance level, easing the burden of learning the reverse diffusion process.

We implemented PriorGrad based on the recently proposed diffusion-based audio generative models [16, 2, 10], and conducted experiments on the LJSpeech [9] dataset. The experimental results demonstrate the potential benefits of PriorGrad, such as a significantly faster model convergence during training, improved perceptual quality, data efficiency, and a reduction in model capacity.

In summary, our contributions are as follows:

- To the best of our knowledge, our study is the first to systemically investigate the effect of using a non-standard Gaussian distribution as the forward diffusion process prior to the conditional generative model.
- Compared to previous non-parametric forward diffusion without any assumption, we show that the model convergence can be significantly accelerated by leveraging the conditional information as the adaptive prior.
- We provide a comprehensive empirical study and analysis of the diffusion model behavior in audio generative models, in both the spectral and waveform domains, and demonstrate the effectiveness of the method.

2 Background

In this section, we describe the basic formulation of the diffusion-based model and provide related studies, along with a description of our contribution with PriorGrad.

Basic formulation Denoising diffusion probabilistic models (DDPM) [7] are recently proposed deep generative models defined by two Markov chains: forward and reverse processes. The *forward process* procedurally destroys the data x_0 into a standard Gaussian x_T , as follows:

$$q(x_{1:T}|x_0) = \prod_{t=1}^T q(x_t|x_{t-1}), \quad q(x_t|x_{t-1}) := \mathcal{N}(x_t; \sqrt{1 - \beta_t}x_{t-1}, \beta_t\mathbf{I}), \quad (1)$$

where $q(x_t|x_{t-1})$ represents the transition probability at the t -th step using a user-defined noise schedule $\beta_t \in \{\beta_1, \dots, \beta_T\}$. Thus, the noisy distribution of x_t is the closed form of $q(x_t|x_0) = \mathcal{N}(x_t; \sqrt{\bar{\alpha}_t}x_0, (1 - \bar{\alpha}_t)\mathbf{I})$, where $\alpha_t := 1 - \beta_t$, $\bar{\alpha}_t := \prod_{s=1}^t \alpha_s$. $q(x_T|x_0)$ becomes a standard Gaussian $\mathcal{N}(x_T; 0, \mathbf{I})$ based on a well-defined noise schedule.

The *reverse process* that procedurally transforms the prior noise into data is defined as follows:

$$p_\theta(x_{0:T}) = p(x_T) \prod_{t=1}^T p_\theta(x_{t-1}|x_t), \quad p_\theta(x_{t-1}|x_t) = \mathcal{N}(x_{t-1}; \mu_\theta(x_t, t), \Sigma_\theta(x_t, t)), \quad (2)$$

where $p(x_T) = \mathcal{N}(x_T; 0, \mathbf{I})$ and $p_\theta(x_{t-1}|x_t)$ corresponds to the reverse of the forward transition probability, parameterized using a deep neural network. We can define the evidence lower bound (ELBO) loss as the training objective of the reverse process:

$$L(\theta) = \mathbb{E}_q \left[\text{KL}(q(x_T|x_0)||p(x_T)) + \sum_{t=2}^T \text{KL}(q(x_{t-1}|x_t, x_0)||p_\theta(x_{t-1}|x_t)) - \log p_\theta(x_0|x_1) \right] \quad (3)$$

As shown in [7], $q(x_{t-1}|x_t, x_0)$ can be represented by Bayes rule as follows:

$$q(x_{t-1}|x_t, x_0) = N(x_{t-1}; \tilde{\mu}(x_t, x_0), \tilde{\beta}_t \mathbf{I}) \quad (4)$$

$$\tilde{\mu}_t(x_t, x_0) := \frac{\sqrt{\bar{\alpha}_{t-1}}\beta_t}{1 - \bar{\alpha}_t} x_0 + \frac{\sqrt{\bar{\alpha}_t}(1 - \bar{\alpha}_{t-1})}{1 - \bar{\alpha}_t} x_t, \quad \tilde{\beta}_t := \frac{1 - \bar{\alpha}_{t-1}}{1 - \bar{\alpha}_t} \beta_t \quad (5)$$

By fixing $p(x_T)$ as a standard Gaussian, $\text{KL}(q(x_T|x_0)||p(x_T))$ becomes constant and is not parameterized. The original framework in [7] fixed $\Sigma_\theta(x_t, t)$ as a constant $\tilde{\beta}_t \mathbf{I}$ and set the standard Gaussian noise ϵ as the optimization target instead of $\tilde{\mu}_t$ by reparameterizing $x_0 = \frac{1}{\sqrt{\bar{\alpha}_t}}(x_t - \sqrt{1 - \bar{\alpha}_t}\epsilon)$ from $q(x_t|x_0)$ to minimize the second and third terms in Eq. (3). Based on this setup, in [7], the authors further demonstrated that we can drop the weighting factor of each term and use a simplified training objective that provides a higher sample quality:

$$L_{\text{simple}}(\theta) := \mathbb{E}_{t, x_0, \epsilon} [\|\epsilon - \epsilon_\theta(x_t, t)\|^2] \quad (6)$$

Related work Since the introduction of the DDPM, there have been a variety of further studies [23, 34], applications [2, 10, 16, 32], and a symbiosis of diffusion [7, 33] and score-based models [35, 36] as a unified view with stochastic differential equations (SDEs) [37]. From an application perspective, several conditional generative models have been proposed. Waveform synthesis models [2, 16] are one of the major applications in which the diffusion model is trained to generate time-domain audio from the prior noise, conditioned on a mel-spectrogram. A diffusion-based decoder has also been applied to text-to-spectrogram generation models [10, 26]. PriorGrad focuses on improving the efficiency of training such methods from the perspective of a conditional generative model. We investigate the potential inefficiency of the current methods which require unfeasibly large computing resources to train and generate high-quality samples.

Studies on formulating an informative prior distribution for deep generative model are not new, and there has been a variety of studies investigating a better prior, ranging from hand-crafted [21, 38], autoregressive [3], vector quantization [27], prior encoder [30], and data-dependent approaches similar to ours [19]. We tackle the problem of training inefficiency of diffusion-based models by crafting better priors in a data-dependent manner, where our method can provide a better trajectory and can reduce spurious modes, enabling more efficient training. Note that there has been a concurrent study conducted on leveraging the prior distribution on the acoustic model, Grad-TTS [26], in which the effectiveness of using the mean-shifted Gaussian as a prior with the identity variance was investigated. Unlike the method in [26], which enforces the encoder output to match the target mel-spectrogram by using an additional encoder loss, our approach augments the forward diffusion prior directly through data and the encoder has no restriction on latent feature representations. In [26], the forward diffusion prior is jointly trained and may induce additional overhead on convergence as the prior changes throughout the training, whereas our method provides guaranteed convergence through the fixed informative prior.

3 Method

We investigate the following intuitive argument: *When we structure the informative prior noise closer to the data distribution, can we improve the efficiency of the diffusion model?* In this section, we

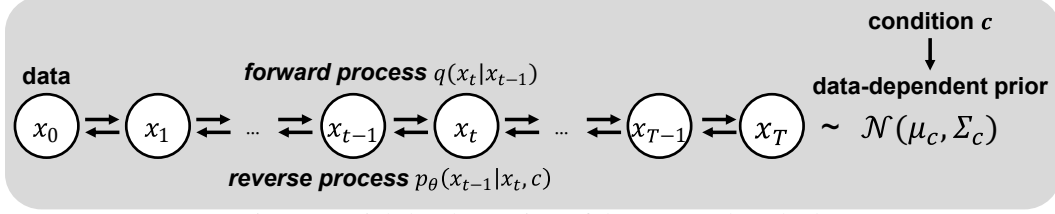


Figure 1: High-level overview of the proposed method.

present a general formulation of PriorGrad, describe training and sampling algorithms, and provide benefits of PriorGrad through a theoretical analysis. PriorGrad offers a generalized approach for the diffusion-based model with the non-standard Gaussian as the prior and can be applied to a variety of applications.

3.1 General Formulation

In this section, we provide a general formulation of the method regarding using the non-standard Gaussian $\mathcal{N}(\mu, \Sigma)$ as the forward diffusion prior. PriorGrad leverages the conditional data to directly compute instance-level approximate priors in an adaptive manner, and provides the approximate prior as the forward diffusion target for both training and inference. Figure 1 presents a visual high-level overview.

We take the same parameterization of μ_θ and σ_θ as in the original DDPM [7] from Section 2, as follows:

$$\mu_\theta(x_t, t) = \frac{1}{\sqrt{\alpha_t}} \left(x_t - \frac{\beta_t}{\sqrt{1 - \alpha_t}} \epsilon_\theta(x_t, t) \right), \quad \sigma_\theta(x_t, t) = \tilde{\beta}_t^{\frac{1}{2}} \quad (7)$$

Assuming that we have access to an optimal Gaussian $\mathcal{N}(\mu, \Sigma)$ as the forward diffusion prior distribution, we have the following modified ELBO objective:

Proposition 1 *Let $\epsilon \sim \mathcal{N}(0, \Sigma)$ and $x_0 \sim q_{data}$. Then, under the parameterization in Eq. (7), the ELBO loss will be*

$$-\text{ELBO} = c + \sum_{t=1}^T \gamma_t \mathbb{E}_{x_0, \epsilon} \|\epsilon - \epsilon_\theta(\sqrt{\alpha_t}(x_0 - \mu) + \sqrt{1 - \alpha_t}\epsilon, t)\|_{\Sigma^{-1}}^2,$$

for some constant c , where $\|x\|_{\Sigma^{-1}}^2 = x^T \Sigma^{-1} x$, $\gamma_t = \frac{\beta_t}{2\alpha_t(1 - \alpha_t)}$ for $t > 1$, and $\gamma_1 = \frac{1}{2\alpha_1}$.

Contrary to the original DDPM, which used $\mathcal{N}(0, I)$ as the prior without any assumption, through Proposition 1, we can train the DDPM models with $\mathcal{N}(\mu, \Sigma)$, whose mean and variance are extracted from the data, as the prior for the forward process. See appendix A.1 for full derivation. Algorithms 1 and 2 describe the training and sampling procedures augmented by the data-dependent prior (μ, Σ) . Because computing the data-dependent prior is application-dependent, in Section 4 and 5, we describe how to compute such prior based on the conditional data on the given task.

Algorithm 1 Training of PriorGrad

repeat
 $(\mu, \Sigma) = \text{data-dependent prior}$
 Sample $x_0 \sim q_{data}, \epsilon \sim \mathcal{N}(0, \Sigma)$
 Sample $t \sim \mathcal{U}(\{1, \dots, T\})$
 $x_t = \sqrt{\alpha_t}(x_0 - \mu) + \sqrt{1 - \alpha_t}\epsilon$
 $\mathcal{L} = \|\epsilon - \epsilon_\theta(x_t, c, t)\|_{\Sigma^{-1}}^2$
 Update the model parameter θ with $\nabla_\theta \mathcal{L}$
until converged

Algorithm 2 Sampling of PriorGrad

$(\mu, \Sigma) = \text{data-dependent prior}$
 Sample $x_T \sim \mathcal{N}(0, \Sigma)$
for $t = T, T-1, \dots, 1$ **do**
 $x_{t-1} = \frac{1}{\sqrt{\alpha_t}}(x_t - \frac{1 - \alpha_t}{\sqrt{1 - \alpha_t}} \epsilon_\theta(x_t, c, t))$
if $t > 1$ **then**
 $x_{t-1} = x_{t-1} + \sigma_t \Sigma^{\frac{1}{2}}$
else
 $x_{t-1} = x_{t-1} + \mu$
end if
end for
return x_0

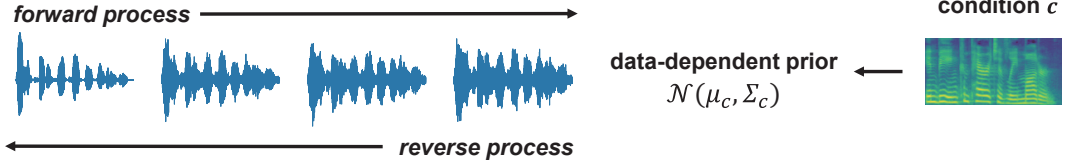


Figure 2: Visual description of PriorGrad for vocoder.

3.2 Theoretical Analysis

In this section, we describe the theoretical benefits of PriorGrad. First, we discuss about the simplified modeling with the following proposition:

Proposition 2 *Let $L(\mu, \Sigma, x_0; \theta)$ denote the $-\text{ELBO}$ loss in Proposition 1. Suppose that ϵ_θ is a linear function. Under the constraint that $\det(\Sigma) = \det(I)$, we have $\min_\theta L(\mu, \Sigma, x_0; \theta) \leq \min_\theta L(0, I, x_0; \theta)$.*

The proposition shows that setting the prior whose covariance Σ aligns with the covariance of data x_0 leads to a smaller loss if we use a linear function approximation for ϵ_θ . This indicates that we can use a simple model to represent the mean of $q(x_{t-1}|x_t)$ under the data-dependent prior, whereas we need to use a complex model to achieve the same precision under a prior with isotropic covariance. The condition $\det(\Sigma) = \det(I)$ means that the two Gaussian priors have equal entropy, which is a condition for a fair comparison.

Second, we discuss the convergence rate. The convergence rate of optimization depends on the condition number of the Hessian matrix of the loss function (denoted as H) [22], that is, $\frac{\lambda_{\max}(H)}{\lambda_{\min}(H)}$, where λ_{\max} and λ_{\min} are the maximal and minimal eigenvalues of H , respectively. A smaller condition number leads to a faster convergence rate. For $L(\mu, \Sigma, x_0; \theta)$, the Hessian is calculated as

$$H = \frac{\partial^2 L}{\partial \epsilon_\theta^2} \cdot \frac{\partial \epsilon_\theta}{\partial \theta} \cdot \left(\frac{\partial \epsilon_\theta}{\partial \theta} \right)^T + \frac{\partial L}{\partial \epsilon_\theta} \cdot \frac{\partial^2 \epsilon_\theta}{\partial \theta^2} \quad (8)$$

Again, if we assume ϵ_θ is a linear function, we have $H \propto I$ for $L(\mu, \Sigma, x_0; \theta)$ and $H \propto \Sigma + I$ for $L(0, I, x_0; \theta)$. It is clear that if we set the prior to be $\mathcal{N}(\mu, \Sigma)$, the condition number of H equals 1, achieving the smallest value of the condition number. Therefore, it can accelerate the convergence. Readers may refer to the appendix A.2 for more details.

4 Application to Vocoder

In this section, we apply PriorGrad to a vocoder model, as visually described in Figure 2.

4.1 PriorGrad for Vocoder

Our formulation of PriorGrad applied to a vocoder is based on WaveGrad [2], where the model synthesizes time-domain waveform conditioned on a mel-spectrogram that contains a compact frequency feature representation of the data. Contrary to the original DDPM, where they used a discrete noise index, the approach in [2] uses a continuous noise level for the forward diffusion process, in a similar spirit to the generalization of the framework as SDEs [37]. With PriorGrad, the network is trained to estimate the noise $\epsilon \sim \mathcal{N}(0, \Sigma)$ given the destroyed signal $\sqrt{\bar{\alpha}_t}x_0 + \sqrt{1 - \bar{\alpha}_t}\epsilon$, conditioned on the continuous noise level $\sqrt{\bar{\alpha}_t}$ and the mel-spectrogram c .

Based on the mel-spectrogram condition, we propose leveraging a normalized frame-level energy of the mel-spectrogram for acquiring data-dependent prior, because it is known that the spectral energy is closely correlated to time-domain waveform variance. First, we compute the frame-level energy by applying roots of sum of exponential to c , where c is the mel-spectrogram from the training dataset. We then normalize the frame-level energy to a range of $(0, 1]$ to acquire the data-dependent variance Σ_c . In this way, we can use the frame-level energy as a proxy of the standard deviation for the waveform data we want to model. We set $\mathcal{N}(0, \Sigma)$ as the forward diffusion prior for each training step by upsampling Σ_c in the frame-level to Σ in the waveform-level using a hop length for the given

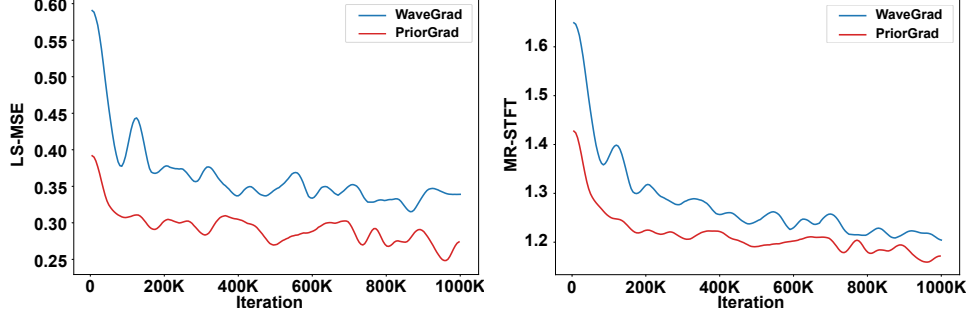


Figure 3: Model convergence result. Left: Log-mel spectrogram mean square error (LS-MSE), Right: Multi-resolution STFT distance (MR-STFT).

vocoder. We chose a zero-mean prior in this setup reflecting the fact that the waveform distribution is zero-mean. In practice, we imposed the minimal standard deviation of the prior to 0.1 through clipping to ensure numerical stability during training. We have tried several alternative sources of conditional information to compute the prior, such as voiced/unvoiced labels and phoneme-level statistics, but they resulted in a worse performance. We justify our choice of using frame-level energy as the prior in the appendix A.3.

Because we are providing more informative prior noise that can have higher mutual information with the data, we additionally hypothesize that we can leverage our modified forward diffusion process by providing a domain-specific auxiliary objective that can provide a further learning signal to the noise estimation network. Inspired by the cycle consistency objective commonly used in other classes of generative models [8, 41], we further propose applying the consistency objective of the estimated noisy signal from the neural network on the entire forward diffusion process. Specifically, given the estimated noise ϵ_θ , we re-sample the noisy signal with $\sqrt{\alpha_t}$ used for sampling x_t as $\tilde{x}_{t,\theta} = \sqrt{\alpha_t}x_0 + \sqrt{1 - \alpha_t}\epsilon_\theta$. Based on the estimated noisy signal $\tilde{x}_{t,\theta}$, we can apply off-shelf auxiliary loss terms with the ground-truth noisy signal x_t with $\mathcal{L}_{cycle}(\tilde{x}_{t,\theta}, x_t)$. In a waveform synthesis, we can apply spectral-domain objectives to guide the trajectory and further reduce spurious mode, which provides a better perceptual quality. We chose the generalized energy distance (GED) [6] as \mathcal{L}_{cycle} because it mitigates the drawbacks of the point-to-point regression used in other spectral losses. We provide the details of the modified training algorithm in the appendix A.4.

4.2 Experimental Setup

We used LJSpeech [9] dataset for all experiments, which is a commonly used open-source 24h speech dataset with 13,100 audio clips from a single female speaker. We used an 80-band mel-spectrogram feature at the log scale from the 22,050Hz volume-normalized speech, with the 1024-point FFT, 80Hz and 8,000Hz low- and high-frequency cutoff, and a hop length of 256. We used 13,000 clips as the training set, 5 clips as the validation set, and the remaining 95 clips as the test set used for an objective and subjective audio quality evaluation.

In the vocoder experiments with PriorGrad, we used the upsampling factor of the U-net [31] of [4, 4, 4, 2, 2] to match a hop length of 256. We used a batch size of 256 with a segment length of 7,168 data points. We followed the publicly available implementation³, where it uses a 15M parameter model with an Adam optimizer [13] and a learning rate of 5.8×10^{-5} for a total of 1M iterations. Training for 1M iterations took approximately 7 days with 4 NVIDIA V100 GPUs.

We used the continuously sampled noise level for training as described in [2], and used the linear reverse beta schedule of 50 iterations ranging from 1×10^{-4} to 5×10^{-2} for fast sampling as well as ensuring a high-quality waveform. We used a coefficient for the auxiliary loss $\lambda_{cycle} = 10^{-2}$, which ensured a numerical scale similar to that of the original ELBO in Eq. (6).

4.3 Experimental Results

We conducted experiments to verify whether our method can learn the reverse diffusion process faster, by comparing the baseline WaveGrad model with $\epsilon \sim \mathcal{N}(0, I)$. First, we present the model

³<https://github.com/ivanvovk/WaveGrad>

Table 1: 5-scale subjective mean opinion score (MOS) results of PriorGrad vocoder with 95% confidence intervals. Text-to-speech results used FastSpeech 2 [28] as an acoustic model.

Type	Method	MOS
	GT	4.31 ± 0.11
Vocoder	GT + WaveGrad [2] (1M)	4.01 ± 0.11
	GT + PriorGrad (300K)	4.06 ± 0.11
Text-to-speech	FastSpeech 2 [28] + WaveGrad [2] (1M)	4.01 ± 0.14
	FastSpeech 2 [28] + PriorGrad (300K)	3.97 ± 0.12

Table 2: CMOS results of PriorGrad vocoder under different training steps.

Method	100K	500K	1M
WaveGrad	0	0	0
PriorGrad	0.297	0.224	0.333

Table 3: Ablation CMOS results of PriorGrad vocoder evaluated on 1M training step.

Method	CMOS
PriorGrad	0
PriorGrad - cycle	-0.131
WaveGrad + cycle	-0.106

convergence result by using a spectral domain loss on the test set to show the fast training of PriorGrad. Second, we provide both objective and subjective audio quality results, where PriorGrad offered the improved quality. Finally, we conduct experiments using a subset of the training data, demonstrating the data efficiency of PriorGrad.

Model convergence We used two widely adopted spectral distances as the proxy of the convergence for the waveform synthesis model: Log-mel spectrogram mean squared error (LS-MSE) and multi-resolution STFT distance (MR-STFT) [40]. We can see from Figure 3 that PriorGrad exhibited a significantly faster spectral convergence compared to the baseline. In the auditory test, we observed that PriorGrad readily removed the background white noise early in training, whereas the baseline needed to learn the entire reverse diffusion process starting from $\epsilon \sim \mathcal{N}(0, I)$ which contains little information. Table 1 shows the 5-scale subjective mean opinion score (MOS) test of PriorGrad. We observed that PriorGrad outperformed the baseline with over 3 times fewer training iterations.

Text-to-speech Table 1 further shows the text-to-speech result using the PriorGrad vocoder. We used the generated mel-spectrogram of a pre-trained FastSpeech 2 [28]. We observed that the text-to-speech results were consistent with the vocoder-only MOS results with the ground-truth mel-spectrogram, which indicates that PriorGrad is robust to potential distributional drifts from the ground-truth mel-spectrogram to that generated by the acoustic model.

Method analysis We provide an in-depth analysis of the model behavior of PriorGrad. As shown in Table 2, PriorGrad consistently achieved higher audio quality under different number of training iterations, where the baseline exhibited higher background white noise particularly for early checkpoints. In Table 3, we provide an ablation study of PriorGrad. Compared to PriorGrad, the ablation model without the cycle loss (PriorGrad - cycle) showed degradation in quality. To show that the cycle consistency loss is not the sole factor for the improved quality, we also trained the baseline WaveGrad model using the same auxiliary objective (WaveGrad + cycle), where the model also showed worse performance than PriorGrad. We can see that PriorGrad offers the best synergy when incorporating domain-specific auxiliary objectives into the diffusion process, because x_T is relatively closer to x_0 in PriorGrad, offering a more meaningful gradient compared to the baseline. PriorGrad also outperformed the baseline on objective speech metrics as shown in Table 4, such as

Table 4: Objective metric results of PriorGrad vocoder experiments. Lower is better.

Method	LS-MSE (\downarrow)	MR-STFT (\downarrow)	MCD (\downarrow)	F ₀ RMSE (\downarrow)
WaveGrad	0.319	1.197	8.876	19.465
PriorGrad	0.270	1.174	7.542	16.936

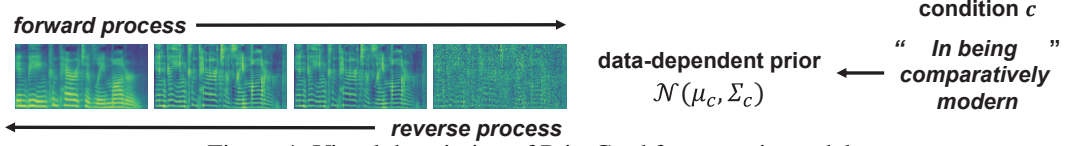


Figure 4: Visual description of PriorGrad for acoustic model.

Mel cepstral distortion (MCD) [17] and F_0 root mean square error (F_0 RMSE), consistent with the subjective quality results.

Data efficiency We further investigated the effectiveness of having an informative prior distribution under a data-constrained setup, where we only used approximately 0.1% of the training dataset (16 audio clips). Although the overall fidelity was reduced, the diffusion model was able to generate highly intelligible waveform. We used the same training setup with 15M parameter models and 1M training steps for WaveGrad and PriorGrad except for the reduced batch size of 16. We observed that the baseline model had a noticeably higher amount of background white noise owing to the availability of less training data, whereas PriorGrad exhibited a better sound quality and had significantly lower artifacts. The subjective CMOS test resulted in a positive gain of +0.282. This suggests that leveraging the informative prior can provide robustness and data efficiency for the training of diffusion-based models.

5 Application to Acoustic Model

In this section, we present the application of PriorGrad to the acoustic models, as visually described in Figure 4.

5.1 PriorGrad for Acoustic Model

The acoustic models generate a mel-spectrogram given a sequence of phonemes with the encoder-decoder architecture. We implement the PriorGrad acoustic model by using the approach in [28] as a feed-forward phoneme encoder, and using a diffusion-based decoder with dilated convolutional layers based on [16]. Note that a similar decoder architecture was used in [10].

To build the adaptive prior, we compute the phoneme-level statistics of the 80-band mel-spectrogram frames by aggregating the frames that correspond to the same phoneme from the training data, where phoneme-to-frame alignment is provided by the Montreal forced alignment (MFA) toolkit [20]. Specifically, for each phoneme, we acquire the 80-dimensional mean and variance from the aggregation of all occurrences in the training dataset. Then, we construct the dictionary of $\mathcal{N}(\mu, \Sigma)$ per phoneme. To use these statistics for the forward diffusion prior, we need to upsample the phoneme-level prior sequence to the frame-level with matching durations. This can be done by jointly upsampling this phoneme-level prior as same as the phoneme encoder output based on the duration predictor [29] module.

Following Algorithm 1, we train the diffusion decoder network with the mean-shifted noisy mel-spectrogram $x_t = \sqrt{\bar{\alpha}_t}(x_0 - \mu) + \sqrt{1 - \bar{\alpha}_t}\epsilon$ as the input. The network estimates the injected noise $\epsilon \sim \mathcal{N}(0, \Sigma)$ as the target. The network is additionally conditioned on the aligned phoneme encoder output. The encoder output is added as a bias term of each dilated convolution layers of the gated residual block with the layer-wise 1×1 convolution.

5.2 Experimental Setup

For the acoustic model experiments, because there are no publicly available implementations of the recently proposed diffusion-based acoustic model [10, 26], we implemented the Transformer encoder architecture based on FastSpeech 2 [28] and the convolutional diffusion decoder architecture based on [10]. We adopted the open-source implementation of the DiffWave architecture⁴ [16] with 12 convolutional layers, similar to [10]. We used the beta schedule with $T = 200$ for training and used the fast reverse sampling algorithm with $T = 6$, as proposed by [16]. We found that the reverse beta

⁴<https://github.com/lmnt-com/diffwave>

Table 5: MOS results of PriorGrad acoustic model with 95% confidence interval.

Method	Small	Large
GT (PWG [40])	4.12 \pm 0.17	
Baseline (300K)	3.69 \pm 0.15	3.86 \pm 0.12
PriorGrad (60K)	3.73 \pm 0.14	3.98 \pm 0.12

Table 6: CMOS results on PriorGrad acoustic model.

Model	Small	Large
Baseline (300K)	0	0
PriorGrad (60K)	0.145	0.408

schedule with $T = 6$ described in [16] performed poorly for the baseline model with $\mathcal{N}(0, I)$. Thus, we applied a grid search over the $T = 6$ reverse schedule for each model, which is a similar approach to that in [2]. This enabled a fair comparative study of each model configuration.

We followed the same training and inference protocols of [28] and used a pre-trained Parallel WaveGAN (PWG) [40] for vocoding. We conducted a comparative study of PriorGrad for acoustic model with a different diffusion decoder network capacity, i.e., a small model with 3M parameters (128 residual channels), and a large model with 10M parameters (256 residual channels). Training for 300K iterations took approximately 2 days on a single NVIDIA P100 GPU. We leave the additional details in the appendix A.5.

5.3 Experimental Results

Model convergence We can see from Table 5 that applying $\mathcal{N}(\mu, \Sigma)$ with PriorGrad significantly accelerated the training convergence and exhibited higher-quality speech for different decoder capacities and training iterations. PriorGrad achieved approximately over 5 times faster convergence compared to the baseline. PriorGrad requires only 60K training iterations to converge, whereas the baseline cannot reach the quality of PriorGrad even after 300K iterations. This is because the training iterations were insufficient for the baseline to learn the entire diffusion trajectory with the standard Gaussian as the prior, leading to poor performance. By contrast, by easing the burden of learning the diffusion process by having access to the phoneme-level informative forward prior, PriorGrad achieved high-quality samples significantly earlier in the training.

Quality improvements We also report that even for the fully converged models, PriorGrad provided additional gain over the baseline. The CMOS results from Table 6 further verified that PriorGrad offers the improved quality even compared to the baseline models trained with longer iterations. This suggests that PriorGrad provides a way to build practical and efficient diffusion-based generative models. This holds a special importance for speech synthesis models, where the efficiency plays a key role in model deployment in realistic environments.

6 Discussion and Conclusion

In this study, we investigated the potential inefficiency of recently proposed diffusion-based model as a conditional generative model within the audio domain. Our method, PriorGrad, directly leverages the rich conditional information and provides an instance-level non-standard adaptive Gaussian as the prior of the forward diffusion process. Through extensive experiments with the recently proposed diffusion-based audio generative models, we showed that PriorGrad achieves a faster model convergence, better denoising of the white background noise, an improved perceptual quality, and data and parameter efficiency. This enables the diffusion-based generative models to be significantly more practical, and real-world applications favor lightweight and efficient models for deployments.

Whereas our focus is on improving the diffusion-based audio generative models, PriorGrad offers a generalized approach to train the diffusion-based model to any data modality. In the image domain, for example, PriorGrad can be applied to image super-resolution tasks [32] by using the patch-wise mean and variance of the low-resolution image to dynamically control the forward/reverse process. We also expect that the method can be used for depth map conditional image synthesis [4], where the depth map can be mapped as the prior variance using the fact that the monocular depth corresponds to the camera focus and visual fidelity between the foreground and background. We leave these applications of PriorGrad for future work.

PriorGrad also has limitations that require further investigation. Although PriorGrad offers a variety of practical benefits as presented, it may also require a well-thought out task-specific design to compute the data-dependent statistics (or its proxy), which may be unsuitable depending on the granularity of the conditional information. Building an advanced approach to enable a more generalized realization of PriorGrad will be an interesting area of future research.

References

- [1] Andrew Brock, Jeff Donahue, and Karen Simonyan. Large scale GAN training for high fidelity natural image synthesis. In *International Conference on Learning Representations*, 2019.
- [2] Nanxin Chen, Yu Zhang, Heiga Zen, Ron J. Weiss, Mohammad Norouzi, and William Chan. Wavegrad: Estimating gradients for waveform generation. In *International Conference on Learning Representations*, 2021.
- [3] Xi Chen, Diederik P. Kingma, Tim Salimans, Yan Duan, Prafulla Dhariwal, John Schulman, Ilya Sutskever, and Pieter Abbeel. Variational lossy autoencoder. In *International Conference on Learning Representations*, 2017.
- [4] Patrick Esser, Robin Rombach, and Björn Ommer. Taming transformers for high-resolution image synthesis. *arXiv preprint arXiv:2012.09841*, 2020.
- [5] Ian Goodfellow, Jean Pouget-Abadie, Mehdi Mirza, Bing Xu, David Warde-Farley, Sherjil Ozair, Aaron Courville, and Yoshua Bengio. Generative adversarial nets. In *Advances in neural information processing systems*, pages 2672–2680, 2014.
- [6] Alexey A Gritsenko, Tim Salimans, Rianne van den Berg, Jasper Snoek, and Nal Kalchbrenner. A spectral energy distance for parallel speech synthesis. *arXiv preprint arXiv:2008.01160*, 2020.
- [7] Jonathan Ho, Ajay Jain, and Pieter Abbeel. Denoising diffusion probabilistic models. In H. Larochelle, M. Ranzato, R. Hadsell, M. F. Balcan, and H. Lin, editors, *Advances in Neural Information Processing Systems*, volume 33, pages 6840–6851. Curran Associates, Inc., 2020.
- [8] Huaibo Huang, Zhihang Li, Ran He, Zhenan Sun, and Tieniu Tan. Introvae: Introspective variational autoencoders for photographic image synthesis. *arXiv preprint arXiv:1807.06358*, 2018.
- [9] Keith Ito and Linda Johnson. The lj speech dataset. <https://keithito.com/LJ-Speech-Dataset/>, 2017.
- [10] Myeonghun Jeong, Hyeongju Kim, Sung Jun Cheon, Byoung Jin Choi, and Nam Soo Kim. Diff-tts: A denoising diffusion model for text-to-speech, 2021.
- [11] Nal Kalchbrenner, Erich Elsen, Karen Simonyan, Seb Noury, Norman Casagrande, Edward Lockhart, Florian Stimberg, Aaron Oord, Sander Dieleman, and Koray Kavukcuoglu. Efficient neural audio synthesis. In *International Conference on Machine Learning*, pages 2410–2419. PMLR, 2018.
- [12] Bahjat Kawar, Gregory Vaksman, and Michael Elad. Stochastic image denoising by sampling from the posterior distribution, 2021.
- [13] Diederik P Kingma and Jimmy Ba. Adam: A method for stochastic optimization. *arXiv preprint arXiv:1412.6980*, 2014.
- [14] Diederik P Kingma and Max Welling. Auto-encoding variational bayes. *arXiv preprint arXiv:1312.6114*, 2013.
- [15] Durk P Kingma and Prafulla Dhariwal. Glow: Generative flow with invertible 1x1 convolutions. In S. Bengio, H. Wallach, H. Larochelle, K. Grauman, N. Cesa-Bianchi, and R. Garnett, editors, *Advances in Neural Information Processing Systems*, volume 31. Curran Associates, Inc., 2018.

- [16] Zhifeng Kong, Wei Ping, Jiaji Huang, Kexin Zhao, and Bryan Catanzaro. Diffwave: A versatile diffusion model for audio synthesis. In *International Conference on Learning Representations*, 2021.
- [17] Robert Kubichek. Mel-cepstral distance measure for objective speech quality assessment. In *Proceedings of IEEE Pacific Rim Conference on Communications Computers and Signal Processing*, volume 1, pages 125–128. IEEE, 1993.
- [18] Junhyeok Lee and Seungu Han. Nu-wave: A diffusion probabilistic model for neural audio upsampling, 2021.
- [19] Zuchao Li, Rui Wang, Kehai Chen, Masso Utiyama, Eiichiro Sumita, Zhuosheng Zhang, and Hai Zhao. Data-dependent gaussian prior objective for language generation. In *International Conference on Learning Representations*, 2019.
- [20] Michael McAuliffe, Michaela Socolof, Sarah Mihuc, Michael Wagner, and Morgan Sonderegger. Montreal forced aligner: Trainable text-speech alignment using kaldi. In *Interspeech*, volume 2017, pages 498–502, 2017.
- [21] Eric Nalisnick and Padhraic Smyth. Stick-breaking variational autoencoders. In *International Conference on Learning Representations*, 2017.
- [22] Yurii Nesterov. *Introductory lectures on convex optimization: A basic course*, volume 87. Springer Science & Business Media, 2003.
- [23] Alex Nichol and Prafulla Dhariwal. Improved denoising diffusion probabilistic models, 2021.
- [24] Aaron Van Oord, Nal Kalchbrenner, and Koray Kavukcuoglu. Pixel recurrent neural networks. In Maria Florina Balcan and Kilian Q. Weinberger, editors, *Proceedings of The 33rd International Conference on Machine Learning*, volume 48 of *Proceedings of Machine Learning Research*, pages 1747–1756, New York, New York, USA, 20–22 Jun 2016. PMLR.
- [25] Aaron van den Oord, Sander Dieleman, Heiga Zen, Karen Simonyan, Oriol Vinyals, Alex Graves, Nal Kalchbrenner, Andrew Senior, and Koray Kavukcuoglu. Wavenet: A generative model for raw audio. *arXiv preprint arXiv:1609.03499*, 2016.
- [26] Vadim Popov, Ivan Vovk, Vladimir Gogoryan, Tasnima Sadekova, and Mikhail Kudinov. Grad-tts: A diffusion probabilistic model for text-to-speech, 2021.
- [27] Ali Razavi, Aaron van den Oord, and Oriol Vinyals. Generating diverse high-fidelity images with vq-vae-2. *arXiv preprint arXiv:1906.00446*, 2019.
- [28] Yi Ren, Chenxu Hu, Xu Tan, Tao Qin, Sheng Zhao, Zhou Zhao, and Tie-Yan Liu. FastSpeech 2: Fast and high-quality end-to-end text to speech. *arXiv preprint arXiv:2006.04558*, 2020.
- [29] Yi Ren, Yangjun Ruan, Xu Tan, Tao Qin, Sheng Zhao, Zhou Zhao, and Tie-Yan Liu. FastSpeech: Fast, robust and controllable text to speech. *arXiv preprint arXiv:1905.09263*, 2019.
- [30] Danilo Rezende and Shakir Mohamed. Variational inference with normalizing flows. In *International Conference on Machine Learning*, pages 1530–1538. PMLR, 2015.
- [31] Olaf Ronneberger, Philipp Fischer, and Thomas Brox. U-net: Convolutional networks for biomedical image segmentation. In *International Conference on Medical image computing and computer-assisted intervention*, pages 234–241. Springer, 2015.
- [32] Chitwan Saharia, Jonathan Ho, William Chan, Tim Salimans, David J. Fleet, and Mohammad Norouzi. Image super-resolution via iterative refinement, 2021.
- [33] Jascha Sohl-Dickstein, Eric A. Weiss, Niru Maheswaranathan, and Surya Ganguli. Deep unsupervised learning using nonequilibrium thermodynamics. In *International Conference on Learning Representations*, 2015.
- [34] Jiaming Song, Chenlin Meng, and Stefano Ermon. Denoising diffusion implicit models. In *International Conference on Learning Representations*, October 2020.

- [35] Yang Song and Stefano Ermon. Generative modeling by estimating gradients of the data distribution. In *Advances in Neural Information Processing Systems*, pages 11895–11907, 2019.
- [36] Yang Song and Stefano Ermon. Improved techniques for training score-based generative models. In Hugo Larochelle, Marc’ Aurelio Ranzato, Raia Hadsell, Maria-Florina Balcan, and Hsuan-Tien Lin, editors, *Advances in Neural Information Processing Systems*, 2020.
- [37] Yang Song, Jascha Sohl-Dickstein, Diederik P Kingma, Abhishek Kumar, Stefano Ermon, and Ben Poole. Score-based generative modeling through stochastic differential equations. In *International Conference on Learning Representations*, 2021.
- [38] Jakub Tomczak and Max Welling. Vae with a vampprior. In *International Conference on Artificial Intelligence and Statistics*, pages 1214–1223. PMLR, 2018.
- [39] Arash Vahdat and Jan Kautz. NVAE: A deep hierarchical variational autoencoder. In *Neural Information Processing Systems (NeurIPS)*, 2020.
- [40] Ryuichi Yamamoto, Eunwoo Song, and Jae-Min Kim. Parallel wavegan: A fast waveform generation model based on generative adversarial networks with multi-resolution spectrogram. In *ICASSP 2020-2020 IEEE International Conference on Acoustics, Speech and Signal Processing (ICASSP)*, pages 6199–6203. IEEE, 2020.
- [41] Jun-Yan Zhu, Taesung Park, Phillip Isola, and Alexei A Efros. Unpaired image-to-image translation using cycle-consistent adversarial networks. In *Proceedings of the IEEE international conference on computer vision*, pages 2223–2232, 2017.

A Appendix

A.1 Derivation of the ELBO Loss

Proposition 1 *Let $\epsilon \sim \mathcal{N}(0, \Sigma)$ and $x_0 \sim q_{data}$. Then, under the parameterization in Eq. (7), the ELBO loss will be*

$$-\text{ELBO} = c + \sum_{t=1}^T \gamma_t \mathbb{E}_{x_0, \epsilon} \|\epsilon - \epsilon_\theta(\sqrt{\bar{\alpha}_t}(x_0 - \mu) + \sqrt{1 - \bar{\alpha}_t}\epsilon, t)\|_{\Sigma^{-1}}^2,$$

for some constant c , where $\|x\|_{\Sigma^{-1}}^2 = x^T \Sigma^{-1} x$, $\gamma_t = \frac{\beta_t}{2\alpha_t(1-\bar{\alpha}_t)}$ for $t > 1$, and $\gamma_1 = \frac{1}{2\alpha_1}$.

Proof:

According to Algorithm 1, the input x_0 is normalized by subtracting its mean μ . In the following, we denote $\tilde{x}_0 = x_0 - \mu$ and $x_t = \sqrt{\bar{\alpha}_t}\tilde{x}_0 + \sqrt{1 - \bar{\alpha}_t}\epsilon$.

According to Equation (3), the ELBO loss is

$$\text{ELBO} = -\mathbb{E}_q \left(\text{KL}(q(x_T|\tilde{x}_0)||p(x_T)) + \sum_{t=2}^T \text{KL}(q(x_{t-1}|x_t, \tilde{x}_0)||p_\theta(x_{t-1}|x_t)) - \log p_\theta(\tilde{x}_0|x_1) \right).$$

Let ϵ_i 's $\overset{i.i.d.}{\sim} \mathcal{N}(0, \Sigma)$. Similarly to the Equation (1), we have $q(x_t|\tilde{x}_0) = \mathcal{N}(x_t; \sqrt{\bar{\alpha}_t}\tilde{x}_0, (1 - \bar{\alpha}_t)\Sigma)$.

By Bayes rule and Markov chain property,

$$\begin{aligned} q(x_{t-1}|x_t, \tilde{x}_0) &= \frac{q(x_t|x_{t-1})q(x_{t-1}|\tilde{x}_0)}{q(x_t|\tilde{x}_0)} \\ &= \frac{\mathcal{N}(x_t; \sqrt{\bar{\alpha}_t}x_{t-1}, \beta_t\Sigma)\mathcal{N}(x_{t-1}; \sqrt{\bar{\alpha}_{t-1}}\tilde{x}_0, (1 - \bar{\alpha}_{t-1})\Sigma)}{\mathcal{N}(x_t; \sqrt{\bar{\alpha}_t}\tilde{x}_0, (1 - \bar{\alpha}_t)\Sigma)} \\ &= (2\pi\tilde{\beta}_t)^{-\frac{d}{2}} \exp \left(-\frac{1}{2\tilde{\beta}_t} \left\| x_{t-1} - \frac{\sqrt{\bar{\alpha}_{t-1}}\beta_t}{1 - \bar{\alpha}_t} \tilde{x}_0 \right\|_{\Sigma^{-1}}^2 \right), \end{aligned}$$

where $\|x\|_{\Sigma^{-1}}^2 = x^T \Sigma^{-1} x$. Therefore,

$$q(x_{t-1}|x_t, \tilde{x}_0) = \mathcal{N} \left(x_{t-1}; \frac{\bar{\alpha}_{t-1}\beta}{1 - \bar{\alpha}_t} \tilde{x}_0 + \frac{\sqrt{\bar{\alpha}_t(1 - \bar{\alpha}_{t-1})}}{1 - \bar{\alpha}_t} x_t, \tilde{\beta}_t \Sigma \right)$$

Then, we calculate each term of the ELBO expansion. The first term is

$$\mathbb{E}_q \text{KL}(q(x_T|\tilde{x}_0)||p(x_T)) = \frac{\bar{\alpha}_T}{2} \mathbb{E}_{\tilde{x}_0} \|\tilde{x}_0\|_{\Sigma^{-1}}^2 - \frac{d}{2} (\bar{\alpha}_T + \log(1 - \bar{\alpha}_T)). \quad (9)$$

The second term is

$$\mathbb{E}_q \text{KL}(q(x_{t-1}|x_t, \tilde{x}_0)||p_\theta(x_{t-1}|x_t)) = \frac{\beta_t}{2\alpha_t(1 - \bar{\alpha}_{t-1})} \mathbb{E}_{\tilde{x}_0, \epsilon} \|\epsilon - \epsilon_\theta(x_t, t)\|_{\Sigma^{-1}}^2. \quad (10)$$

Finally, we have

$$\mathbb{E}_q \log p_\theta(\tilde{x}_0|x_1) = -\frac{1}{2} \log(2\pi\beta_1)^d \det(\Sigma) - \frac{1}{2\alpha_1} \mathbb{E}_{\tilde{x}_0, \epsilon} \|\epsilon - \epsilon_\theta(x_1, 1)\|_{\Sigma^{-1}}^2. \quad (11)$$

Combining Equation (9), (10) and (11) together, we can get the result in the Proposition.

A.2 Theoretical Benefits of PriorGrad

Proposition 2 *Let $L(\mu, \Sigma, x_0; \theta)$ denote the $-\text{ELBO}$ loss in Proposition 1. Suppose that ϵ_θ is a linear function. Under the constraint that $\det(\Sigma) = \det(I)$, we have $\min_\theta L(\mu, \Sigma, x_0; \theta) \leq \min_\theta L(0, I, x_0; \theta)$.*

Proof: We use $L(\mu, \Sigma, x_0; \theta)$ to denote -ELBO. According to Equation (9), (10) and (11), we have

$$\begin{aligned} L(\mu, \Sigma, x_0; \theta) &= \frac{\bar{\alpha}_T}{2} \mathbb{E}_{x_0} \|\tilde{x}_0\|_{\Sigma^{-1}}^2 + \frac{1}{2} \log \det(\Sigma) + \sum_{t=1}^T \gamma_t \mathbb{E}_{x_0, \epsilon} \|\epsilon - \epsilon_\theta(\sqrt{\bar{\alpha}_t} \tilde{x}_0 + \sqrt{1 - \bar{\alpha}_t} \epsilon, t)\|_{\Sigma^{-1}}^2 \\ &\quad + \frac{d}{2} \log(2\pi\beta_1) - \frac{d}{2} (\bar{\alpha}_T + \log(1 - \bar{\alpha}_T)), \end{aligned}$$

where $\tilde{x}_0 = x_0 - \mu$. We assume that $\epsilon_\theta(\cdot)$ is a scalar function with parameter freedom d , i.e., $\epsilon_\theta(\sqrt{\bar{\alpha}_t} \tilde{x}_0 + \sqrt{1 - \bar{\alpha}_t} \epsilon, t) = \theta(\sqrt{\bar{\alpha}_t} \tilde{x}_0 + \sqrt{1 - \bar{\alpha}_t} \epsilon)$, where $\theta \in \mathbb{R}^{d \times d}$ with constraint $\tilde{\theta} = Q\theta = \text{diag}(\tilde{\theta}_1, \dots, \tilde{\theta}_d)$ and Q is the eigenmatrix for Σ^{-1} , i.e., $\Sigma^{-1} = Q^T \tilde{\Sigma}^{-1} Q$ with $\tilde{\Sigma}^{-1} = \text{diag}(\frac{1}{\sigma_1}, \dots, \frac{1}{\sigma_d})$. For the term $\sum_{t=1}^T \gamma_t \mathbb{E}_{x_0, \epsilon} \|\epsilon - \theta(\sqrt{\bar{\alpha}_t} \tilde{x}_0 + \sqrt{1 - \bar{\alpha}_t} \epsilon)\|_{\Sigma^{-1}}^2$, we have

$$\begin{aligned} &\sum_{t=1}^T \gamma_t \mathbb{E}_{x_0, \epsilon} \|\epsilon - \theta(\sqrt{\bar{\alpha}_t} \tilde{x}_0 + \sqrt{1 - \bar{\alpha}_t} \epsilon)\|_{\Sigma^{-1}}^2 \\ &= \sum_{t=1}^T \gamma_t \mathbb{E}_{x_0, \epsilon} \|Q(\epsilon - \theta(\sqrt{\bar{\alpha}_t} \tilde{x}_0 + \sqrt{1 - \bar{\alpha}_t} \epsilon))\|_{\tilde{\Sigma}^{-1}}^2 \\ &= \sum_{j=1}^d \left(\frac{1}{\sigma_j} \sum_{t=1}^T \gamma_t \left(\sigma_j + (1 - \bar{\alpha}_t) \tilde{\theta}_j^2 \sigma_j + \bar{\alpha}_t \tilde{\theta}_j^2 \sigma_j - 2\sigma_j \sqrt{1 - \bar{\alpha}_t} \tilde{\theta}_j \right) \right) \\ &= \sum_{j=1}^d \left(\frac{1}{\sigma_j} \sum_{t=1}^T \gamma_t \left(\sigma_j + \tilde{\theta}_j^2 \sigma_j - 2\sigma_j \sqrt{1 - \bar{\alpha}_t} \tilde{\theta}_j \right) \right) \\ &= \sum_{j=1}^d \left(\sum_{t=1}^T \gamma_t \left(1 + \tilde{\theta}_j^2 - 2\sqrt{1 - \bar{\alpha}_t} \tilde{\theta}_j \right) \right) \end{aligned} \tag{12}$$

where the second equation is established by taking expectation of x_0 and ϵ . The above equation will achieve its minimum at $\tilde{\theta}_j = \frac{\sum_{t=1}^T \gamma_t \sqrt{1 - \bar{\alpha}_t}}{\sum_{t=1}^T \gamma_t}$, $\forall j$, and the minimum is $\sum_{j=1}^d \left(\sum_{t=1}^T \gamma_t - \frac{(\sum_{t=1}^T \gamma_t \sqrt{1 - \bar{\alpha}_t})^2}{\sum_{t=1}^T \gamma_t} \right)$.

For $L(0, I, x_0; \theta)$, we have

$$\begin{aligned} L(0, I, x_0; \theta) &= \frac{\bar{\alpha}_T}{2} \mathbb{E}_{x_0} \|x_0\|^2 + \frac{1}{2} \log \det(I) + \sum_{t=1}^T \gamma_t \mathbb{E}_{x_0, \epsilon} \|\epsilon - \theta(\sqrt{\bar{\alpha}_t} x_0 + \sqrt{1 - \bar{\alpha}_t} \epsilon, t)\|^2 \\ &\quad + \frac{d}{2} \log(2\pi\beta_1) - \frac{d}{2} (\bar{\alpha}_T + \log(1 - \bar{\alpha}_T)), \end{aligned}$$

Similarly, we can get the minimum of $\sum_{t=1}^T \gamma_t \mathbb{E}_{x_0, \epsilon} \|\epsilon - \theta(\sqrt{\bar{\alpha}_t} x_0 + \sqrt{1 - \bar{\alpha}_t} \epsilon, t)\|^2$ with a diagonal θ is $\sum_{j=1}^d \left(\sum_{t=1}^T \gamma_t - \frac{(\sum_{t=1}^T \gamma_t \sqrt{1 - \bar{\alpha}_t})^2}{\sum_{t=1}^T \gamma_t (1 - \bar{\alpha}_t + \bar{\alpha}_t \sigma_j)} \right)$. Under the condition that $\det(\Sigma) = \det(I)$, we have the minimum of $\sum_{j=1}^d \left(\sum_{t=1}^T \gamma_t - \frac{(\sum_{t=1}^T \gamma_t \sqrt{1 - \bar{\alpha}_t})^2}{\sum_{t=1}^T \gamma_t (1 - \bar{\alpha}_t + \bar{\alpha}_t \sigma_j)} \right)$ (over all possibilities of $(\sigma_1, \dots, \sigma_d)$) will be $\sum_{j=1}^d \left(\sum_{t=1}^T \gamma_t - \frac{(\sum_{t=1}^T \gamma_t \sqrt{1 - \bar{\alpha}_t})^2}{\sum_{t=1}^T \gamma_t} \right)$ (by solving the constrained minimization problem). Thus, we get the result in the Proposition.

Remark: From Equation (12), we have the second order derivative of $L(\mu, \Sigma, x_0; \theta)$ with respect to θ_j equals $\sum_{t=1}^T \gamma_t$ for all $j = 1, \dots, d$. Thus the condition number of the Hessian matrix equals 1. Similarly, the second order derivative of $L(0, I, x_0; \theta)$ with respect to θ_j equals $\sum_{t=1}^T \gamma_t (1 - \bar{\alpha}_t + \bar{\alpha}_t \sigma_j)$. Thus the Hessian matrix equals $c_1 I + c_2 \Sigma$ with $c_1 = \sum_{t=1}^T \gamma_t (1 - \bar{\alpha}_t)$ and $c_2 = \sum_{t=1}^T \gamma_t \bar{\alpha}_t$, whose condition number is no less than 1.

A.3 Exploration on the Conditional Information Source of PriorGrad Vocoder

In this section, we provide further discussion regarding the source of the conditional information for constructing PriorGrad vocoder and empirical justification of selecting the frame-level spectral energy

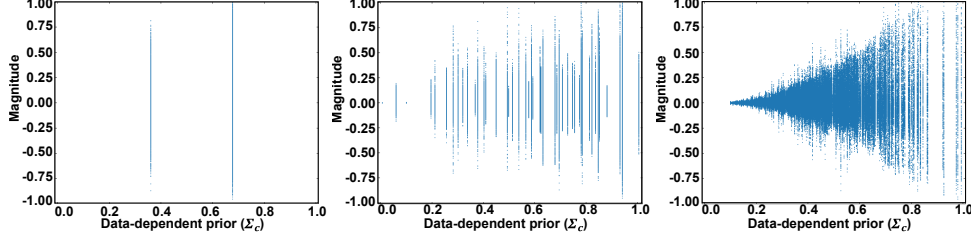


Figure 5: Scatter plots of waveform audio signals from the test set under different choices of the conditional information for PriorGrad vocoder. Left: V/UV label-based prior. Middle: Phoneme label-based prior. Right: Energy-based prior.

as the prior. Considering the waveform synthesis model as a vocoder, the main application of such model is a spectrogram inversion module of the text-to-speech pipeline. That is, the vocoder model is usually combined with the acoustic model as a front-end, where the acoustic model generates the mel-spectrogram based on text input. FastSpeech 2 [28] demonstrated a significant improvement in the quality of the acoustic model leveraged by carefully designed additional speech-related features for fine-grained supervision, such as voiced/unvoiced (V/UV) label obtained from F0 contours, or phoneme-to-frame alignment labels. We explored V/UV or phoneme labels as alternative sources of information for constructing the prior.

Figure 5 shows scatter plots of the waveform audio clip from the test set corresponding to the standard deviation labels assigned by Σ_c acquired from the training set. Because the V/UV label is binary, we can only assign two different prior variances to the waveform distribution, which is an overly coarse assumption of the data distribution. Phoneme-level prior can offer more fine-grained approximate prior. However, we found that the variance statistics acquired from the training set is misaligned with the unobserved waveform, where the actual variance can be significantly different to the target prior, leading to an inconsistent result. The frame-level spectral energy for PriorGrad exhibited the best alignment of the label and the unobserved waveform data and demonstrated consistent results in quality.

A.4 Extended Training Algorithm of PriorGrad Vocoder

Algorithm 3 describes a detailed training algorithm of PriorGrad vocoder with the cycle consistency auxiliary objective. We used a publicly available implementation of the GED [6] because it provided better quality compared to other spectral losses, although PriorGrad can apply any off-shelf distance metric as the objective. The trained model uses the same algorithm for sampling in Algorithm 2. We note that the additional operations included in the cycle consistency objective have negligible overheads during training.

Algorithm 3 Full training algorithm of PriorGrad vocoder with cycle consistency auxiliary loss

repeat

$(\mu, \Sigma) = \text{data-dependent prior}$

Sample $x_0 \sim q_{data}$, $(\epsilon, \epsilon') \sim \mathcal{N}(0, \Sigma)$ and $s \sim \text{Uniform}(\{1, \dots, S\})$

Sample $\sqrt{\bar{\alpha}_t} \sim \text{Uniform}(l_{s-1}, l_s)$

Sample $x_t = \sqrt{\bar{\alpha}_t}(x_0 - \mu) + \sqrt{1 - \bar{\alpha}_t}\epsilon$ and $x'_t = \sqrt{\bar{\alpha}_t}(x_0 - \mu) + \sqrt{1 - \bar{\alpha}_t}\epsilon'$

Compute $\mathcal{L}_{diffusion} = \|\epsilon - \epsilon_\theta(x_t, c, \sqrt{\bar{\alpha}_t})\|_{\Sigma^{-1}}^2$

Sample $\tilde{x}_{t,\theta} = \sqrt{\bar{\alpha}_t}(x_0 - \mu) + \sqrt{1 - \bar{\alpha}_t}\epsilon_\theta(x_t, c, \sqrt{\bar{\alpha}_t})$ and $\tilde{x}'_{t,\theta} = \sqrt{\bar{\alpha}_t}(x_0 - \mu) + \sqrt{1 - \bar{\alpha}_t}\epsilon'_\theta(x'_t, c, \sqrt{\bar{\alpha}_t})$

Compute $\mathcal{L}_{cycle} = \text{GED}(x_t, \tilde{x}_{t,\theta}, \tilde{x}'_{t,\theta})$

Update the model parameter θ with gradient $\nabla_\theta(\mathcal{L}_{diffusion} + \lambda_{cycle}\mathcal{L}_{cycle})$

until converged

A.5 Additional Details of PriorGrad Acoustic Model

In this section, we describe additional details of the experimental settings of the PriorGrad acoustic model. The feed-forward Transformer-based phoneme encoder has 11.5M parameters trained with

Table 7: Sampling noise schedule used for PriorGrad acoustic model experiments obtained by a grid search method [2].

Method	Sampling Noise Schedule
Baseline (Small)	$\{3 \times 10^{-4}, 2 \times 10^{-3}, 3 \times 10^{-2}, 8 \times 10^{-2}, 8 \times 10^{-1}, 9 \times 10^{-1}\}$
Baseline (Large)	$\{1 \times 10^{-4}, 4 \times 10^{-3}, 3 \times 10^{-2}, 8 \times 10^{-2}, 8 \times 10^{-1}, 9 \times 10^{-1}\}$
PriorGrad (Small)	$\{3 \times 10^{-4}, 8 \times 10^{-3}, 2 \times 10^{-2}, 3 \times 10^{-2}, 8 \times 10^{-1}, 9 \times 10^{-1}\}$
PriorGrad (Large)	$\{3 \times 10^{-4}, 6 \times 10^{-3}, 3 \times 10^{-2}, 4 \times 10^{-2}, 8 \times 10^{-1}, 9 \times 10^{-1}\}$

the Adam optimizer with the learning rate schedule identically described in [28]. The diffusion decoder is simultaneously trained with the same training configurations.

For a fair comparative study between different diffusion models, we searched for the best performing baseline model with $\mathcal{N}(0, I)$ first, then applied PriorGrad to this baseline. We applied $T = 200$ for the diffusion decoder with a linearly spaced beta schedule ranging from 1×10^{-4} to 5×10^{-2} . We found that 1×10^{-4} to 2×10^{-2} used for waveform domain in [16] performed poorly for the baseline, where the model failed to capture the high-frequency details of the mel-spectrogram. This indicates that the optimal training noise schedule can be different, depending on the data domain. On the contrary, PriorGrad’s performance was similar under different choices of training noise schedules, suggesting that PriorGrad also features robustness regarding designing the noise schedules for model training.

The baseline model’s performance was sensitive to the choice of the fast sampling noise schedule with $T = 6$. Thus, we applied a fine-grained grid search over every possible combination of the monotonically increasing $T = 6$ betas based on the L1 loss between the model prediction and the target from the validation set. We applied the following range for the grid search:

$$\{1, 2, 3, 4, 5, 6, 7, 8, 9\} \times 10^{-4}, 10^{-3}, 10^{-2}, 10^{-2}, 10^{-1}, 10^{-1} \quad (13)$$

Note that a similar technique is used in [2]. We found that setting relatively high betas at the last steps was important for the quality of the baseline model, whereas PriorGrad was significantly more robust to the choice of the noise schedule. Table 7 shows the optimal beta schedules for each model configuration from the grid search method.

A.6 Audio Samples Demo Webpage

We provide a demo webpage of the audio samples: <https://speechresearch.github.io/priorgrad/>